Results in Engineering 27 (2025) 105978

Contents lists available at ScienceDirect

Results in Engineering

journal homepage: www.sciencedirect.com/journal/results-in-engineering

Research paper

Optimizing turning parameters of duralumin nano Cr_2C_3–MoS_2 using ANN and MOORA: A multi-objective approach

Ramesh Vellaichamy [a], Pugazhenthi Rajagopal [a,*], Ajith Arul Daniel Selsam Chandradoss [a], A. Geetha Selvarani [b]

[a] Department of Mechanical Engineering, Vels Institute of Science, Technology & Advanced Studies, Chennai 600117, India
[b] Department of Civil Engineering, Vel Tech Rangarajan Dr. Sagunthala R&D Institute of Science and Technology, India

ARTICLE INFO

Keywords:
Chromium carbide
Duralumin
Accoustic emission
Vibration
Molybdeneum disulphide

ABSTRACT

This investigation presents a comprehensive parametric optimization study for the precision machining of duralumin matrix composites reinforced with hybrid nano-scale particles comprising chromium carbide (Cr_2C_3) and molybdenum disulfide (MoS_2). The composite material was synthesized via liquid metallurgy stir casting methodology, incorporating 5 wt% nano-Cr_2C_3 as the primary reinforcement phase and 2 wt% MoS_2 as a solid lubricant additive to enhance tribological characteristics and machinability. The experimental framework employed a Taguchi L_{27} orthogonal array design to systematically investigate the influence of critical machining parameters like cutting velocity, feed rate, and depth of cut on multiple response characteristics including surface roughness (Ra), tool vibration amplitude, and acoustic emission (AE) intensity. The multi-response optimization strategy integrated advanced computational intelligence techniques, specifically utilizing a Levenberg–Marquardt backpropagation artificial neural network (LM-BP-ANN) for predictive modeling and enhanced accuracy in handling non-linear optimization problems. The Multi-Objective Optimization on the basis of Ratio Analysis (MOORA) technique was implemented to establish the optimal parametric combination that simultaneously minimizes surface roughness, vibration, and acoustic emission. Statistical analysis of variance (ANOVA) was performed on the MOORA-derived performance index (Y_i) it revealed that feed rate exhibits the most pronounced influence on the combined response characteristics, contributing 71.05 % to the total variation. The optimization results indicate that the optimal machining conditions for achieving minimal surface roughness, vibration amplitude, and acoustic emission are: feed rate of 0.20 mm/rev, depth of cut of 0.75 mm, and cutting speed of 80 m/min.

1. Introduction

The development of lightweight materials is highly desired by the automotive and aerospace sectors to improve mechanical properties and the strength-to-weight ratio [1]. Compared to current alloys, Metal Matrix Composites (MMCs) can significantly reduce the weight of components and offer a high strength-to-weight ratio [2,3]. They can also serve as substitutes for metals used in fabricating components in the automotive industry [4].

Modern manufacturing processes have overcome many challenges associated with high-strength materials, including the formation of complex shapes, more precise surface features, higher levels of precision, reduced waste and additional processes, and extended production durations [5]. Even at elevated temperatures, Hybrid Metal Matrix Composites (HMMCs) outperform both polymer and metal matrix composites due to their multiple reinforcement particles and higher strength-to-stiffness ratios [6].

The production of MMCs utilizes various methods, including liquid infiltration, powder metallurgy, stir casting, and squeeze casting. Among these techniques, stir casting is the most economical for fabricating composites [7]. Several manufacturing processes can be used to shape the developed composites for industrial applications, with turning being a traditional method of producing the final product. When properly optimized, the technique enables the tool to operate with minimal vibration and achieve low surface roughness.

During turning operations, vibration and surface quality depend on various factors such as tool and component material, feed rate, spindle

* Corresponding author.
E-mail addresses: rameshaarakavya@gmail.com (R. Vellaichamy), pugal4@gmail.com (P. Rajagopal), ajithdanny1989@gmail.com (A.A.D.S. Chandradoss), drgeethaselvarani@veltech.edu.in (A.G. Selvarani).

https://doi.org/10.1016/j.rineng.2025.105978
Received 8 April 2025; Received in revised form 22 June 2025; Accepted 24 June 2025
Available online 25 June 2025
2590-1230/© 2025 The Authors. Published by Elsevier B.V. This is an open access article under the CC BY license (http://creativecommons.org/licenses/by/4.0/).

Nomenclature

Abbreviation	Full Form
ANN	Artificial Neural Network
MOORA	Multi-Objective Optimization on the basis of Ratio Analysis
CNC	Computer Numerical Control
MMC	Metal Matrix Composite
HMMC	Hybrid Metal Matrix Composite
Ra	Surface Roughness
AE	Acoustic Emission
ANOVA	Analysis of Variance
MCDM	Multi-Criteria Decision Making
MADM	Multiple Attribute Decision Making
RSM	Response Surface Methodology
L27	Taguchi Orthogonal Array (27 runs)
S/N Ratio	Signal-to-Noise Ratio
Cr2C3	Chromium Carbide
MoS2	Molybdneum Di Sulphide

Table 1
Design of experiments.

Factor	Name	Units	Coded Low	Coded High	Mean	Std. Dev.
A	Cutting speed	m/min	−1 ↔ 80.00	+1 ↔ 160.00	120.00	33.28
B	Feed	m/min	−1 ↔ 0.20	+1 ↔ 0.30	0.2500	0.0416
C	Cutting depth	Mm	−1 ↔ 0.25	+1 ↔ 0.75	0.5000	0.2080

Table 2
L27 orthogonal array with response parameters.

	Factor A	Factor B	Factor C	Response 1	Response 2	Response 3
Run	Cutting speed	Feed	Cutting depth	Ra	Vibration	Acoustic Emission
Unit	m/min	mm/min	mm			
1	80	0.2	0.25	1.46	7.54	0.82
2	80	0.2	0.25	0.88	7.73	1.02
3	80	0.2	0.25	1.17	8.74	0.83
4	80	0.25	0.5	1.74	10.76	0.92
5	80	0.25	0.5	1.75	11.78	0.75
6	80	0.25	0.5	2.14	12.63	0.78
7	80	0.3	0.75	3.15	9.46	0.85
8	80	0.3	0.75	3.09	10.51	0.63
9	80	0.3	0.75	3.1	11.95	0.77
10	120	0.2	0.5	1.11	11.68	1.18
11	120	0.2	0.5	1.5	11.21	1.3
12	120	0.2	0.5	1.21	12.65	1.25
13	120	0.25	0.75	2.16	11.11	1.03
14	120	0.25	0.75	2.08	12.12	0.82
15	120	0.25	0.75	2.09	13.79	1.01
16	120	0.3	0.25	3.43	17.38	1.28
17	120	0.3	0.25	3.7	19.14	1.31
18	120	0.3	0.25	2.95	18.12	1.28
19	160	0.2	0.75	0.92	7.83	1.36
20	160	0.2	0.75	1.19	10.14	1.3
21	160	0.2	0.75	1.18	8.26	1.5
22	160	0.25	0.25	2.12	17.24	1.8
23	160	0.25	0.25	2.49	18.65	1.97
24	160	0.25	0.25	2.39	18.37	1.77
25	160	0.3	0.5	4.02	18.34	1.73
26	160	0.3	0.5	3.76	16.54	1.75
27	160	0.3	0.5	3.66	18.65	1.54

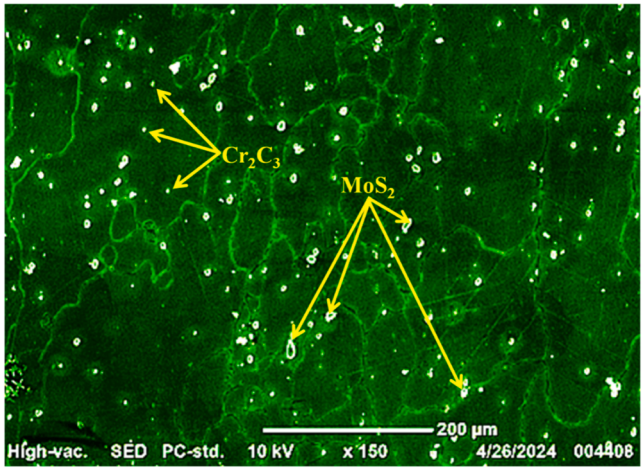

Fig. 1. SEM image of the Duralumin composite with 5 % Cr_2C_3 and 2 % MoS_2.

speed, depth of cut, coolant, tool construction, tool nose radius, and tool edge angles [8]. Establishing an adequate relationship among tool life, cutting conditions, tool geometry, and material properties is essential. However, such analysis is challenging due to the complex nature of the machining process, which involves high temperatures, strains, strain rates, and insufficient data.

Moreover, the ideal cutting conditions can enhance surface smoothness and reduce costs and production time [9]. In recent years, researchers have focused on optimizing cutting parameters during machining processes to reduce both surface roughness and vibration [10]. In a study on the adhesion level between the cutting tool and workpiece during turning, a model with extensive degrees of freedom was proposed for chatter prediction. It highlighted the significant effects of workpiece cross-section and tool overhang on process stability during orthogonal turning [11].

Incorporating ceramic reinforcements into aluminum alloys improves the overall properties of composite materials. M.K. Surappa [12] found that damage-resistant properties such as fracture toughness and ductility needed enhancement. Kumar et al. [13] studied the effect of various matrix materials (Al6061 and Al7075) and reinforcements (SiC and Al_2O_3) and found that increasing filler content and the volume fraction of particles improved the composite's microhardness.

Surface roughness increased during the machining of Al_2O_3 particle-reinforced aluminum (Al2024) composites using coated carbide tools. Researchers found that cutting velocity depends 20.8 % on surface roughness for the A356/20/SICP-T6 composite [14]. In his work with Al2024/Al_2O_3 composites, Kok et al. [15] observed that the sharpness of the tool, regardless of whether the carbide was coated or not, primarily influenced surface roughness. Increasing the tool's feed speed reduced the surface roughness of the workpiece.

Sahin et al. [16] significantly influenced wear behavior through pin-on-disc tests, using Taguchi techniques and ANOVA in their statistical analyses. The percentage of reinforcement weight influenced wear, and the right amount of reinforcement helped achieve an even distribution through the stirring process in the made composites. Optimizing process parameters is crucial for understanding the impact of factors and evaluating their significance in experimental research.

Furthermore, Shirvanimoghaddam et al. [17] reported that the hardness and tensile strength of aluminum alloy composites reinforced with B_4C, TiB_2, and $ZrSiO_4$ particles improved by up to 52 % and 125 %, respectively. Using Taguchi L27 orthogonal arrays, Alagarsamy et al. [18] conducted a study involving three process variables: depth of cut, speed, and feed rate. ANOVA and signal-to-noise ratio analysis guided the measurement of the material removal rate and machining time during the turning operations of aluminum alloy 7075 using tungsten carbide tools. The results showed that cutting speed significantly

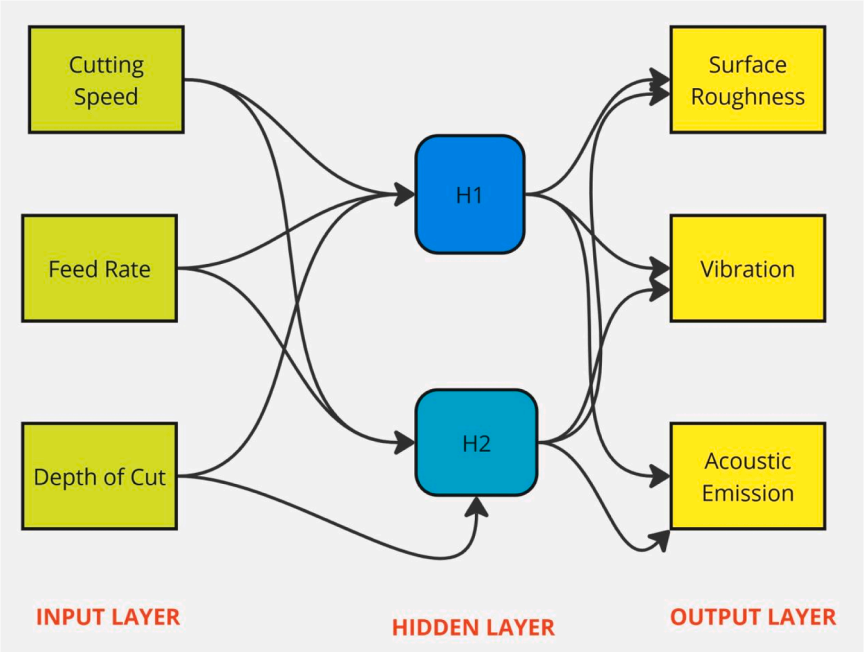

Fig. 2. Three-layer artificial neural networks (ANN) architecture.

influenced lower machining time and higher material removal rate.

Due to their many benefits, such as increased accuracy, reduced time and cost, and the ability to model complex nonlinear relationships between process parameters and output predictions of Artificial Neural Networks (ANNs) are highly applicable for such analyses [19]. Typically, two main procedures are used when machining new materials: predicting response variables and optimizing process parameters, while also studying the influence of process parameters on responses. Predicting response parameters from experimental data is vital and commonly done using regression equations [20].

However, Muthukrishnan and Davim [21] demonstrated that the ANN method is more effective than regression equations in predicting relationships in the AMMC machining process, especially for surface roughness and input parameters. Sahoo et al. [22] used RSM and ANN to develop predictive models and optimize cutting parameters, including 3D surface plots. In their experiments with AISI 1040 steel using coated carbide tools under dry conditions, the RSM model achieved an R^2 value of 0.99, indicating a strong model fit. Both ANN and RSM accurately predicted Ra, but the ANN model performed better.

In another study, ANN and RSM were used to analyze the effects of cutting parameters on tangential cutting force (Fz), cutting power (Pc), and surface roughness (Ra) during the turning of POM C polymer. The results indicated that feed rate had the greatest impact on Ra (66.41 %), followed by cutting speed and depth of cut. Cutting depth primarily influenced Fz and Pc, with feed rate being the next most significant factor. Additionally, ANN was found to be a more robust and reliable method than RSM, based on the coefficients of determination (R^2) from the developed models [23].

Nowadays, various Multi-Criteria Decision Making (MCDM) techniques are widely used to select the best materials and composites. For example, selecting materials for structural epoxy composites is crucial. Many researchers apply MCDM and Multiple Attribute Decision Making (MADM) techniques to rank materials based on multiple performance characteristics. Senthil et al. [24] selected wire-cut electrical discharge machining settings using a combined AHP and MOORA analysis. The AHP-MOORA technique can also be employed to determine the optimal combination of machining parameters for minimizing tool wear, improving surface quality, and enhancing overall machining performance [25,26].

The current study sets itself apart by using an Artificial Neural Network (ANN) trained using the Levenberg–Marquardt backpropagation algorithm, whereas many previous studies have concentrated on the optimization of machining parameters and prediction of surface roughness using techniques like regression analysis and Taguchi methods. This study uses the nonlinear learning capabilities of artificial neural networks (ANN) to more precisely predict machining responses, such as surface roughness, under varied turning conditions of hybrid metal matrix composites (HMMCs), in contrast to previous approaches that mainly depend on linear or statistical models. Furthermore, the current approach offers a more adaptable and accurate substitute for conventional modeling techniques by combining a various of process parameters and experimental data to create a robust prediction model. This method improves knowledge and control of the intricate interactions involved in machining advanced composite materials in addition to increasing prediction accuracy.

This research study is distinctive because it takes a holistic approach to optimizing the turning process of a novel hybrid metal matrix composite made using the economical stir casting method. Duralumin reinforces the composite with 5 % Cr_2C_3 and 2 % of MoS_2 nanoparticles. In machining investigations, this combination of reinforcements has not been investigated before, especially when it comes to decreasing surface roughness, tool vibration, and acoustic emission all at once. The study combines the MOORA (Multi-Objective Optimization based on Ratio Analysis) method with Artificial Neural Network (ANN) modeling using the Levenberg–Marquardt backpropagation algorithm, allowing for accurate predictions and optimization of multiple outcomes at once. In contrast to earlier research that frequently focused on single-response optimization, this study uses a multi-criteria decision-making approach to identify the best cutting parameters for enhanced machining performance.

2. Methodology

2.1. Material used

Duralumin is the primary matrix material employed in these experimental investigations. It is an alloy of aluminum mixed with magnesium, manganese, and copper. This composition contains aluminum at

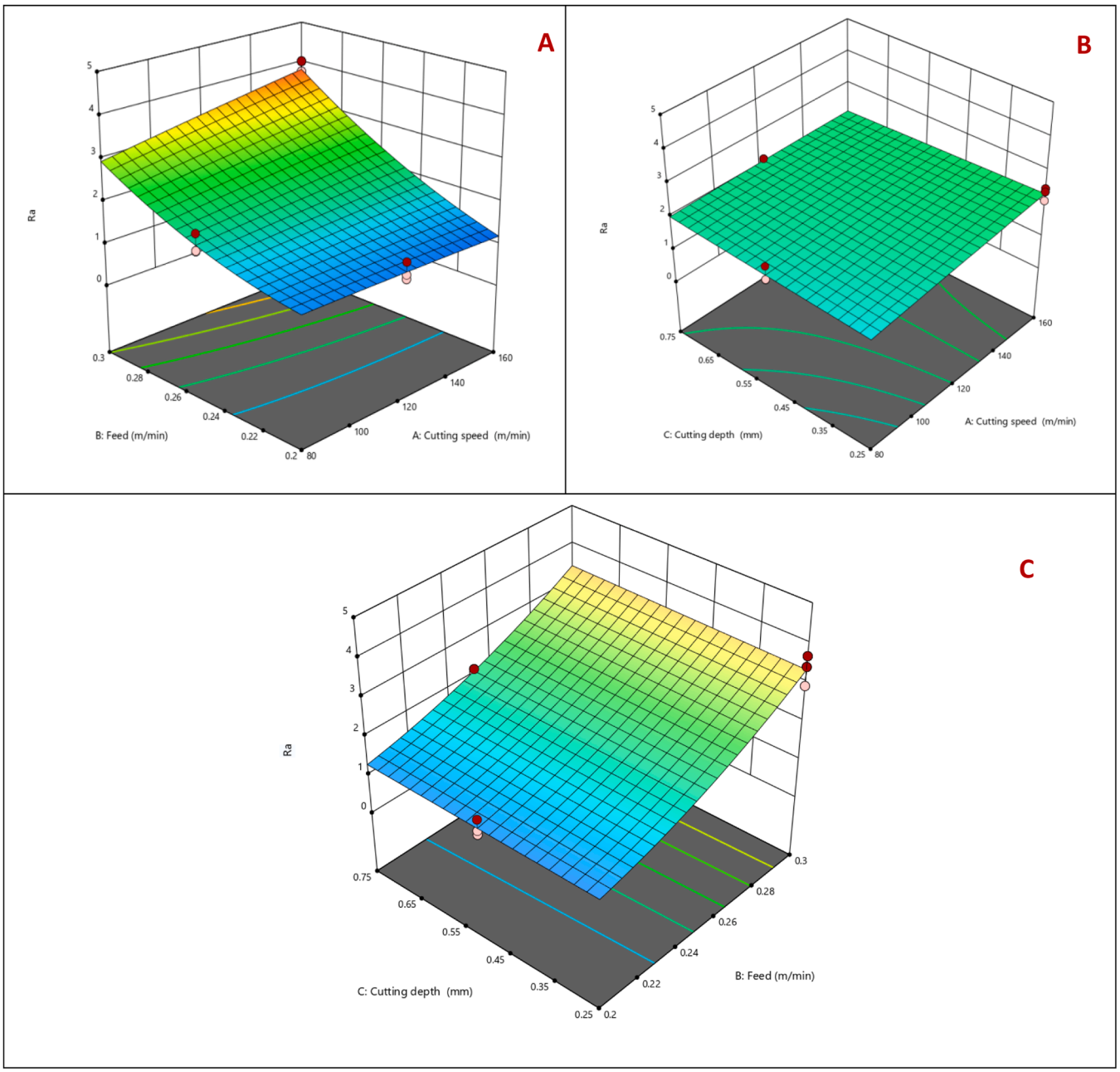

Fig. 3. Contour plot for input parameters VS Surface roughness.

91–95 % by weight, with copper at 3.8–4.9 % and magnesium at 1.2–1.8 % as the prime alloying elements. Nanochromium carbide (Cr_2C_3) serves as the main reinforcing material. MoS_2 is added as secondary reinforcement with a weight percentage of 2 %. Molybdenum disulfide (MoS_2) possesses remarkable chemical and thermal stability its low abrasion characteristics and it is often used as a solid lubricant.

2.2. Conduct of experiment

The Duralumin/Cr_2C_3 & MoS_2 hybrid composite was fabricated via stir casting technique. The reinforcement was heated for 20 min at 450 °C before casting. After preheating the reinforcement, the Duralumin was melted in a graphite crucible at 650 °C. After that, the reinforcement and Duralumin matrix were mixed together, and magnesium was added at a rate of 2 % to the Duralumin base to prevent oxidation. The casting samples underwent a high-speed turning operations utilizing a computer numerical control (CNC) turning center (ECOTURN-25) [20]. The dimensions of casting samples used in the turning process were 25 mm in diameter with a length of 150 mm. A 1616H11 tool holder joined with an uncoated carbide insert 332-SF H13A cutting tool was operated during the turning processes. The turning process occurred within a dry environment. Surface roughness (SR) measurements of the turned casting samples were carried out using a surface roughness tester (Mitutoyo SJ-210) [27]. The vibration of the composites was measured by using tri-axial accelerometer. The electrical noise signals were eliminated through appropriate filtering procedures.

2.3. Design of experiments

Taguchi design of experiments was adapted for the turning operation of the developed composites. The cutting speed, feed rate and depth of cut were chosen as input parameters based on the three levels and three

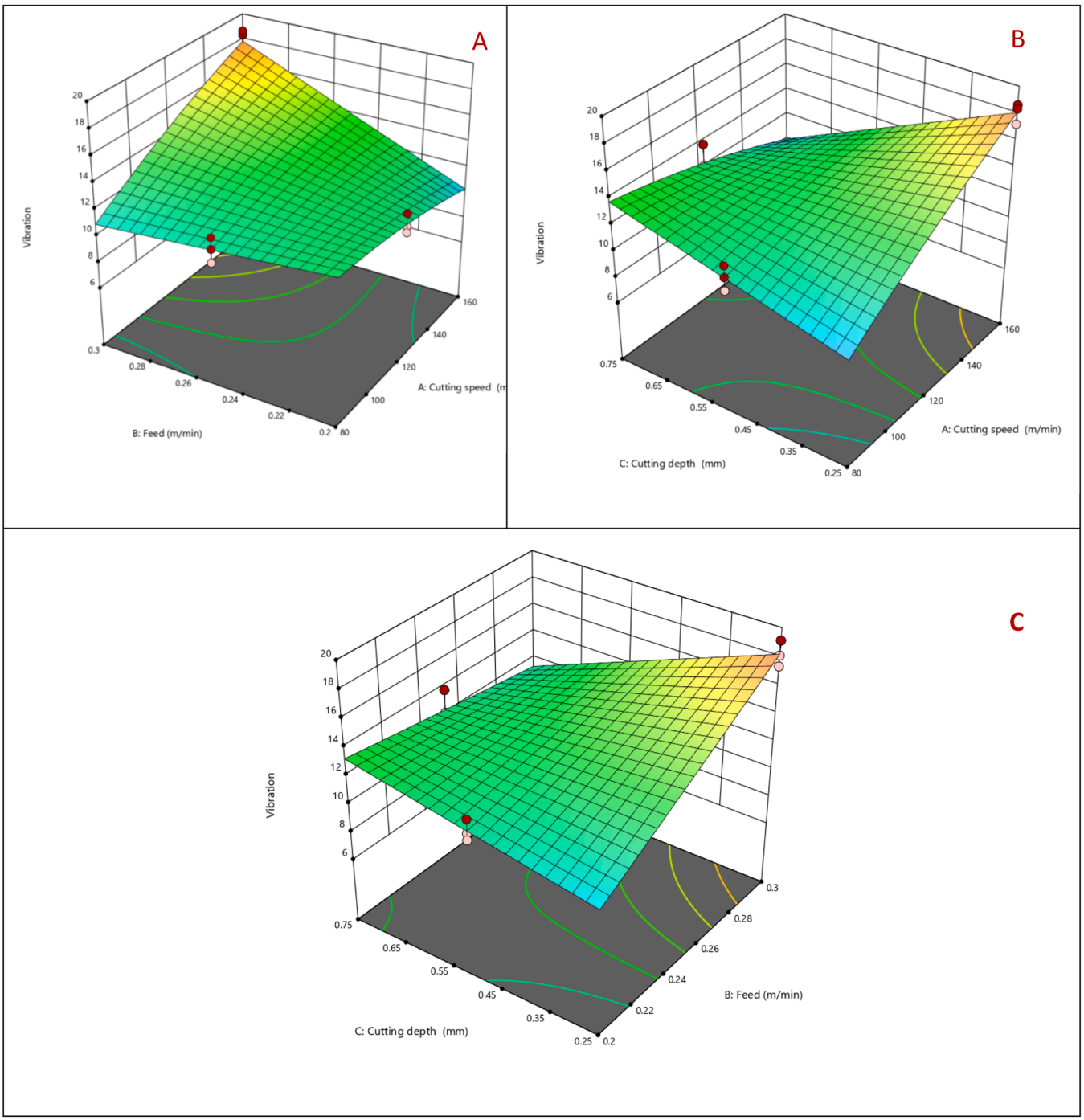

Fig. 4. Contour plot for input parameters VS Vibration.

factors an L27 orthogonal array was chosen for conduct the experiment as shown in Table 1. The results obtained from conducting the experiment for the response parameters i.e., surface roughness, vibration and acoustic emission are shown in Table 2.

2.4. Characterization of the composites

Fig. 1 shows the SEM image of the composite containing 5 % Cr2C3 and 2 % MoS_2, the image captured at 10,000X magnification with 5.00 kV beam voltage, reveals both smooth and rough regions. The darker areas likely represent the matrix material, while the brighter scattered particles are presumed to be the Cr_2C_3 and MoS_2 reinforcements. The reinforcement particles exhibit relatively uniform distribution of the reinforcement particles, though some clustering is observed in certain regions. The surface topography shows some deformation and material displacement, which is Characteristic of wear surfaces. The presence of MoS_2 likely contributes to the formation of a lubricating film, while the Cr_2C_3 particles appear to be well-embedded in the matrix, providing wear resistance. The scale bar indicates 1 μm, showing the micro-scale features of the wear surface. Overall, the microstructure indicates effective integration between the matrix and reinforcement materials.

2.5. Development of ANN modelling

A computational model that considers the components and structure of organic brain systems is called an artificial neural network (ANN).

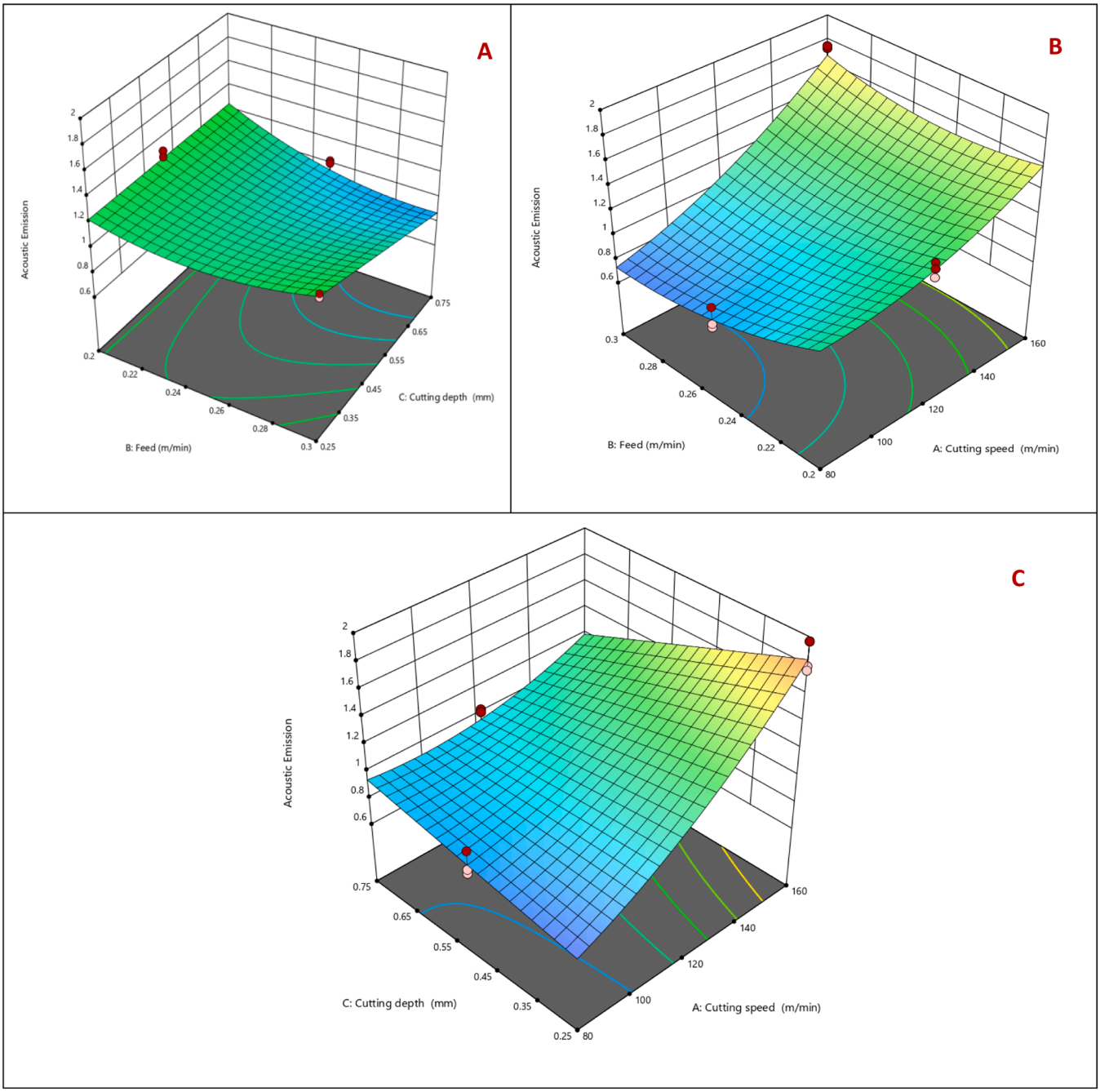

Fig. 5. Contour plot for input parameters VS Acoustic Emission.

The term "neural networks" refers to frameworks that are brain-inspired and aimed at imitating how humans learn. In addition to input and output layers, neural systems frequently have hidden layers made up of units that transform data into something the output layer can use [28]. These tools help reveal complex patterns or large numbers of specifications that exceed human capabilities, enabling machines to learn and understand. Given that a neural system adapts—or learns, if you will—in response to input and output, the data flowing through the system impacts the ANN's structure. Fig. 2 demonstrates a three-layer artificial neural networks (ANN) architecture. Cutting speed, feed rate, and cut depth are the input neurons, while surface roughness, vibration, and acoustic emission are the output neurons. The system uses the back propagation algorithm to train on both input and output values, performing training and validation using 27 experimental datasets.

2.6. *Multi-objective optimization on the basis of ratio analysis method*

The technique of concurrently maximizing two or more competing criteria (objectives) under certain limitations is known as multi-objective optimization. Increasing revenue and lowering expenses for multi-objective optimization problems typically involve optimizing performance and limiting fuel consumption of a vehicle, minimizing weight while increasing the strength of a certain technical component, or some combination of these [29].

Making decisions in a real-time industrial setting is made significantly more challenging by the diverse interests and principles of decision-makers. The objective (criteria) of a decision-making problem must be quantifiable, and each potential solution must have measurable results. Certain criteria (objectives) have contradictory values; some are advantageous (maximum values are wanted), while others are not ad-

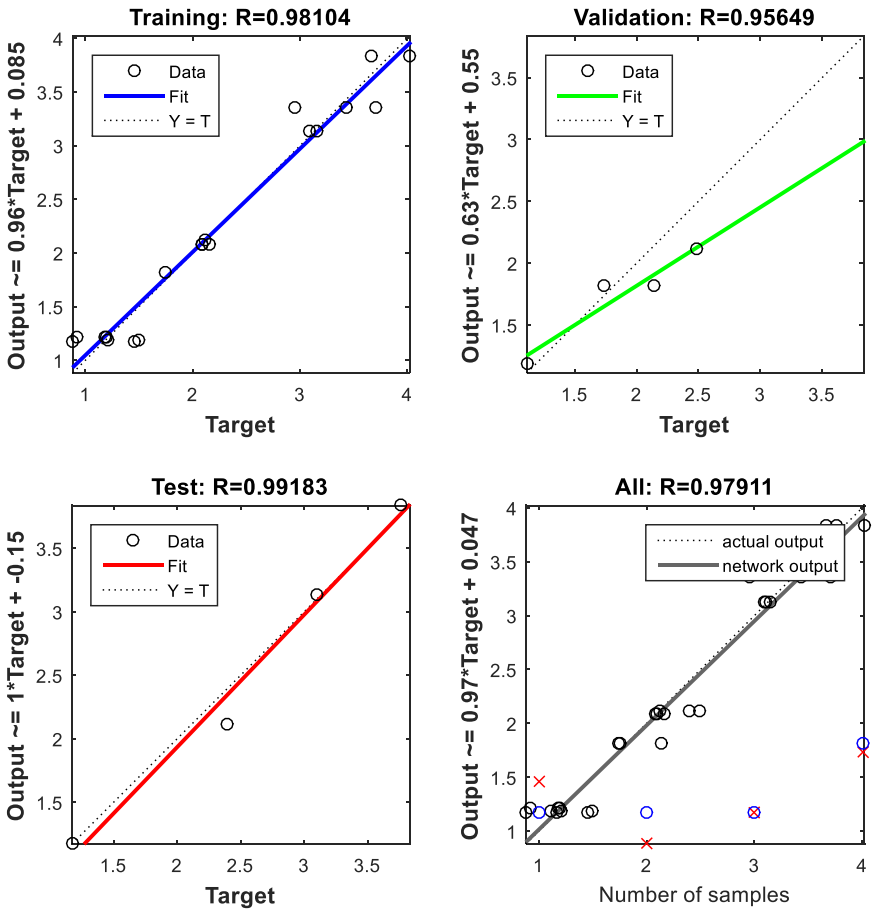

Fig. 6. ANN model for predicting input machining parameters.

vantageous (minimum criteria values are always favored). Using a set of accessible options, the multi-objective optimization based on ratio analysis (MOORA) approach ranks or chooses one or more options by considering both non-beneficial and advantageous objectives (criteria).

$$A = \begin{bmatrix} a_{11} & a_{12} & \dots & \dots & a_{1n} \\ a_{21} & a_{22} & \dots & \dots & a_{2n} \\ \dots & \dots & \dots & \dots & \dots \\ \dots & \dots & \dots & \dots & \dots \\ a_{m1} & a_{m2} & \dots & \dots & a_{mn} \end{bmatrix} \quad (1)$$

Performances among different alternatives are represented using the values a_{ij} where 'i' represents the specific alternative and 'j' denotes the criterion and m stands for total alternatives while n indicates total criteria.

$$a_{ij}^{*} = \frac{a_{ij}}{\sum_{i=1}^{m} a_{ij}} \quad (2)$$

Where a_{ij} variable represents a normalized performance score between zero and one which indicates the i^{th} alternative's criteria value on j^{th} criterion

It is occasionally seen that suggested the following normalizing process, the normalized value for a particular criterion exceeds one whenever a decision matrix contains a very big value for that criterion.

$$a_{ij}^{*} = a_{ij} \Big/ \left[\sum_{i=1}^{m} a_{ij}^{2}\right]^{1/2} \quad (j = 1, 2, \dots, n) \quad (3)$$

Therefore, it is advised to use Eq. (3) to reduce the maximum criteria value to less than one. As stated in the accompanying expression, the MOORA method requires performance normalization with added points for beneficial criteria and then subtracted points for non-beneficial criteria.

$$b_i = \sum_{j=1}^{g} a_{ij}^{*} - \sum_{j=g+1}^{n} a_{ij}^{*} \quad (4)$$

The assessing value of the *ith* option with regarding to all criteria is represented by 'b_i' while 'g' designates the total amount of criteria to be maximized alongside (n g) for the criteria to be minimized.

$$X_i = Min_{(i)}\left(Max_{(i)}\left|Z_i a_{ij}^{*}\right|\right) \quad (5)$$

The selection option providing the highest assessment value is considered the best choice after arranging options from highest to lowest value. The selection process among potential alternatives should follow an orderly ranking system based on bi values.

3. Results and discussion

The analysis reveals distinct relationships that connect the parameters utilized during machining operations to their measured performance results. The tool removes more material per revolution when the feed rate rises from 0.2 to 0.3 mm/rev, which results in deeper tool marks and a rougher surface because of the higher scallop height. Because higher speeds generate larger dynamic forces, tool deflection, and potential resonance, especially under higher feed circumstances, cutting speed, especially in the maximum range significantly affects vibration [30]. As cutting speed goes up, more friction, chip formation, and changes in the material structure create short bursts of sound, leading to a steady rise in acoustic emission, which is highest between 1.50 and 1.97 at 160 m/min. These results demonstrate a trade-off between preserving surface quality and increasing material removal rates;

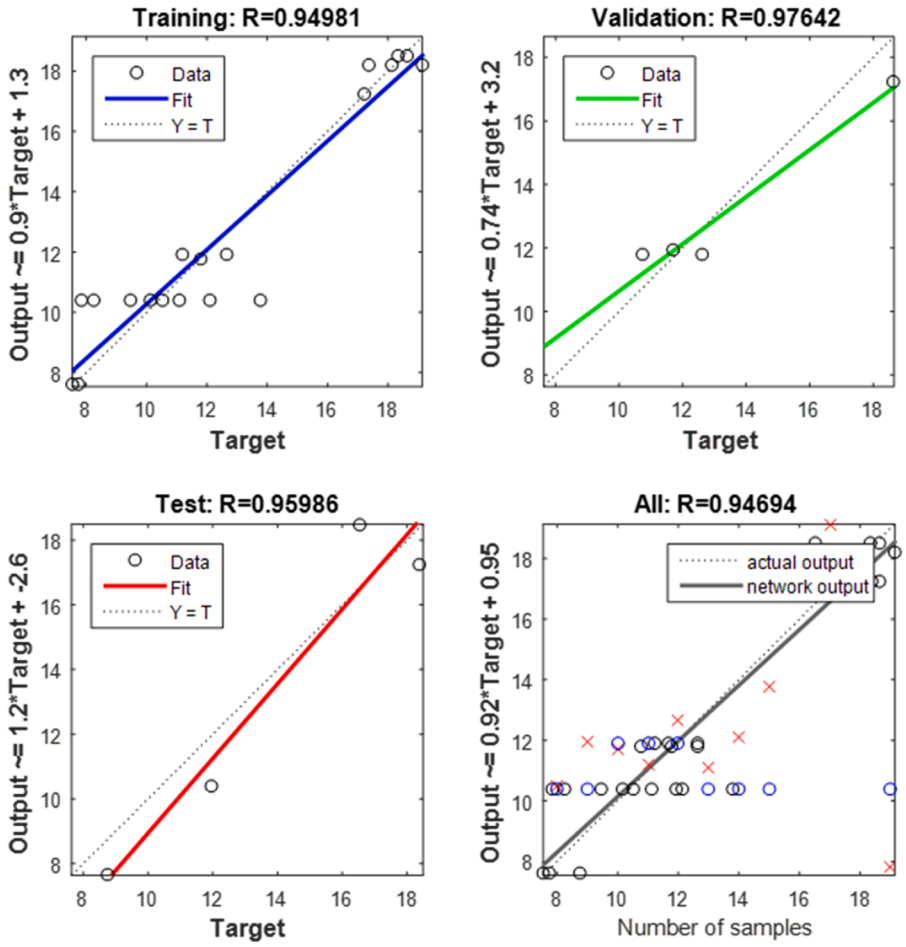

Fig. 7. ANN Correlation coefficients (R-values).

high cutting speeds need to be carefully managed to limit vibration and AE, when low feed rates enhance surface finish. Based on the intended machining result, productivity and stability must be balanced while optimizing machining process parameters.

The 3D surface plot represents the mutual interaction between feed rate, depth of cut, and cutting speed that affects surface roughness, as displayed in Fig. 3. The system exhibits surface plot data that shows the relationship between cutting speed and feed parameters for stable depth of cut measurements under machining force conditions. The surface plots revealed that feed rate was the factor with the greatest impact on machining force. The plot also showed that when the feed rate increases from 2.5 mm/min to 3 mm/min, the machining force increases. This occurs because the region of contact between the tool and the composite workpiece material expands with an increase in feed rate. The machining force increases during the machining process due to accelerated material removal, which is enabled by the larger contact zone area [31]. Fig. 3B shows the surface plot of machining force versus cutting speed and depth of cut. A correlation was found between machining force and depth of cut. For higher cutting speeds, low feed rates, and shallower cuts, it was discovered that the machining force was minimal. It was observed that the machining force increased as the feed rate and depth of cut increased, and that the machining force decreased at low feed rates and shallow depths of cut. This occurs because the material removal rate increases with higher feed rates and depth of cut, which in turn increases the machining power required to remove chips from the workpiece material [32]. Additionally, the contact area between the workpiece material and the cutting insert expands with increased feed rate. The cutting tool experiences minimal resistance at low feed rates, but the workpiece material's resistance to the tool inserts increases at high speeds, resulting in increased friction and cutting force.

Vibration measurements for a 0.50 mm depth of cut showed a decrease corresponding to spindle speed increases. However, the vibration values for both cutting tools at 0.25 mm and 0.75 mm depth of cut showed no regular pattern, as shown in Fig. 4A. The lowest natural frequency was obtained with a conventional cutting tool at 120 mm/min spindle speed and 0.50 mm depth of cut, while the highest vibration amplitude was obtained at 120 mm/min spindle speed and 0.50 mm depth of cut for a cutting tool with holes in the toolholder. Fig. 4B shows that, for a conventional cutting tool, the vibration value at 0.25 mm depth of cut decreases proportionally with increasing spindle speed; however, the vibration pattern for the modified cutting tool is irregular. In 160 mm/min spindle speed for the cutting tool with holes in the toolholder produced the maximum vibration value at the same tool overhang [33]. Increased depth of cut can lead to higher tool vibration, and this phenomenon is commonly observed in turning of developed composites as shown in Fig. 4C. Tool vibration can have several negative effects, including reduced tool life, poor surface finish, and potential damage to the workpiece and machine tool [34]. A deeper cut typically results in higher cutting forces. The tool must remove more material, resulting in greater resistance and force on the cutting edge, which can cause the tool to deflect or vibrate due to these increased forces.

The performance of router tools was monitored online using an acoustic emission (AE) sensor to ascertain the correlation between the AE signal and the machining duration for various tool geometries. According to the analysis, a router tool with a flat cutting edge performs better because it produces lower cutting forces and achieves a superior surface finish with no delamination on the trimmed edges of the cutting tool. Fig. 5A shows the contour relationship between depth of cut and

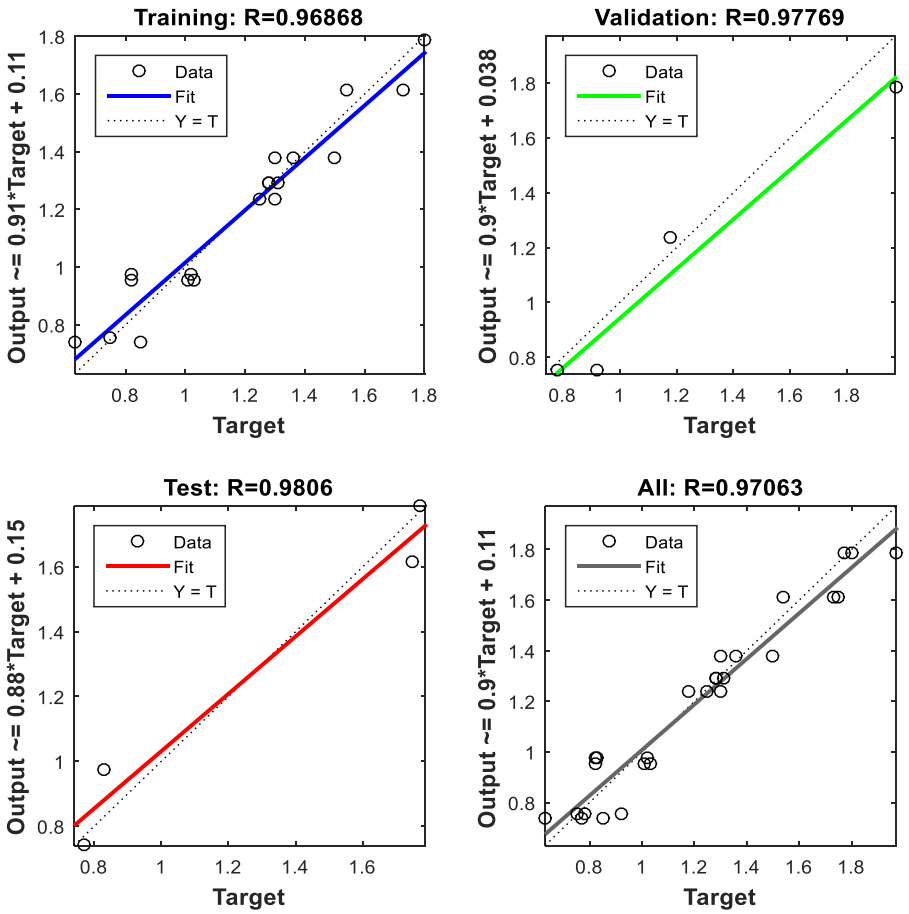

Fig. 8. ANN predicted acoustic emission value based on machining parameters.

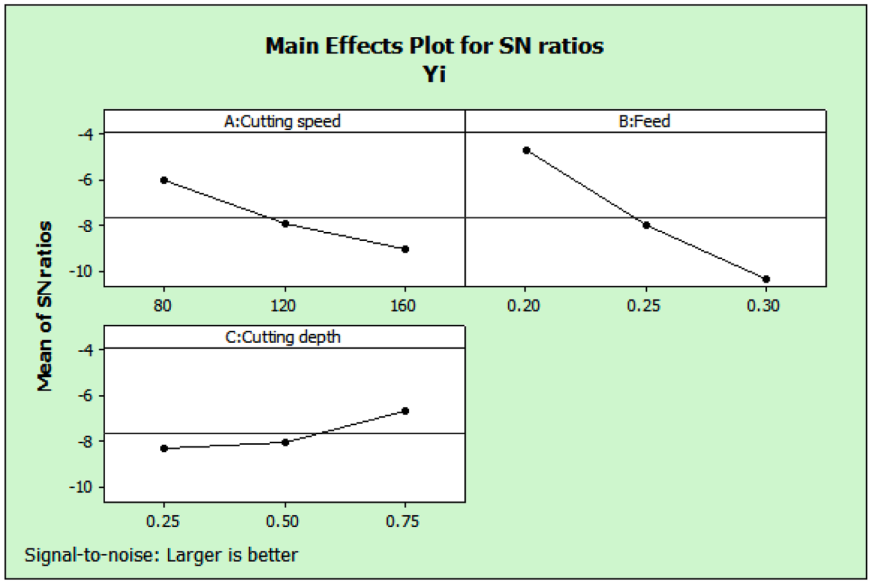

Fig. 9. S-N ratio graph for Yi.

feed rate with respect to acoustic emission. As the depth of cut escalates from 0.5 mm and the feed rate increases from 0.25 mm/min, there is a corresponding acoustic emission of 1.2 v^2/S. The rapid energy release in localized areas of deforming materials under damage conditions creates transient elastic waves known as acoustic emission [35]. The rate of material removal from the workpiece increases in direct proportion to feed rate according to Fig. 5C. This can affect the chip formation process, leading to different types of chips being produced, such as longer or more tightly curled chips. Changes in chip formation can influence the acoustic emission characteristics of the machining process [36]. Increasing the depth of cut can affect the dynamic behavior of the machining system, leading to changes in vibration and resonance

Table 3
MOORA results with square of Ai.

Ra	Vibration	Acoustic Emission	Square of Ai		
1.46	7.54	0.82	2.1316	56.8516	0.6724
0.88	7.73	1.02	0.7744	59.7529	1.0404
1.17	8.74	0.83	1.3689	76.3876	0.6889
1.74	10.76	0.92	3.0276	115.7776	0.8464
1.75	11.78	0.75	3.0625	138.7684	0.5625
2.14	12.63	0.78	4.5796	159.5169	0.6084
3.15	9.46	0.85	9.9225	89.4916	0.7225
3.09	10.51	0.63	9.5481	110.4601	0.3969
3.1	11.95	0.77	9.61	142.8025	0.5929
1.11	11.68	1.18	1.2321	136.4224	1.3924
1.5	11.21	1.3	2.25	125.6641	1.69
1.21	12.65	1.25	1.4641	160.0225	1.5625
2.16	11.11	1.03	4.6656	123.4321	1.0609
2.08	12.12	0.82	4.3264	146.8944	0.6724
2.09	13.79	1.01	4.3681	190.1641	1.0201
3.43	17.38	1.28	11.7649	302.0644	1.6384
3.7	19.14	1.31	13.69	366.3396	1.7161
2.95	18.12	1.28	8.7025	328.3344	1.6384
0.92	7.83	1.36	0.8464	61.3089	1.8496
1.19	10.14	1.3	1.4161	102.8196	1.69
1.18	8.26	1.5	1.3924	68.2276	2.25
2.12	17.24	1.8	4.4944	297.2176	3.24
2.49	18.65	1.97	6.2001	347.8225	3.8809
2.39	18.37	1.77	5.7121	337.4569	3.1329
4.02	18.34	1.73	16.1604	336.3556	2.9929
3.76	16.54	1.75	14.1376	273.5716	3.0625
3.66	18.65	1.54	13.3956	347.8225	2.3716
WEIGHT					
0.468	0.368	0.164	5.934962963	185.25	1.59232963

frequencies. These changes can influence the generation and propagation of acoustic emission waves.

3.1. ANN analysis

The surface roughness results for evaluating the predictive performance of an artificial neural network (ANN) model trained for L27 parameter prediction are shown in Fig. 6. The figure includes four subplots representing different datasets: Training, Validation, Test, and Overall performance. The plots compare the target values against the model's predicted values, with the correlation coefficient (R) indicating the strength of the relationship. The training set shows a high correlation ($R = 0.98496$), while both the validation and test sets achieve perfect correlations ($R = 1$), demonstrating excellent generalization. The overall dataset maintains a strong correlation ($R = 0.98641$), confirming the model's accuracy. The fitted regression lines closely follow the ideal relationship, and the minor deviations in slope and intercept indicate minimal bias and error. These results suggest that the ANN model effectively predicts the L27 parameters with high precision and reliability [39].

Fig. 6 shows the performance evaluation of an ANN model for predicting the machining parameters, presented in four separate subplots. The plots demonstrate the correlation between target (actual) values and predicted outputs for vibration. The top-left plot shows the training data with $R = 0.94981$, indicating a strong correlation between predicted and actual values. The top-right plot displays the validation results with $R = 0.97642$, suggesting even better model performance on the validation set. The bottom-left plot presents the test results with $R = 0.95986$, demonstrating consistent performance on unseen data.

Fig. 7 shows that the correlation coefficients (R-values) are close to 1, indicating a strong linear relationship between the predicted and actual values. The regression equations suggest that the model predicts outputs with slight deviations, as evidenced by slopes close to 0.9 and small intercepts. The graph indicates that while the model captures the trend well, minor variations exist due to data noise or model limitations. Fig. 8 shows the ANN predicted acoustic emission values based on machining parameters. Overall, the ANN model demonstrates good accuracy and generalization for predicting acoustic emission based on machining parameters [37].

3.2. Regression equation

The mathematical model for developed composites is shown in Eq. (5),6 & 7

Table 4
Normalized decision matrix and rank.

Normalized Decision Xij			Weight and normalized			Yi	RANK
0.684931507	0.132625995	1.219512195	0.320547945	0.048806366	0.2	0.569354311	5
1.136363636	0.129366106	0.980392157	0.531818182	0.047606727	0.160784314	0.740209223	1
0.854700855	0.114416476	1.204819277	0.4	0.042105263	0.197590361	0.639695625	3
0.574712644	0.092936803	1.086956522	0.268965517	0.034200743	0.17826087	0.48142713	10
0.571428571	0.084889643	1.333333333	0.267428571	0.031239389	0.218666667	0.517334627	9
0.46728972	0.079176564	1.282051282	0.218691589	0.029136975	0.21025641	0.458084974	12
0.317460317	0.105708245	1.176470588	0.148571429	0.038900634	0.192941176	0.380413239	17
0.323624595	0.095147479	1.587301587	0.151456311	0.035014272	0.26031746	0.446788043	14
0.322580645	0.083682008	1.298701299	0.150967742	0.030794979	0.212987013	0.394749734	16
0.900900901	0.085616438	0.847457627	0.421621622	0.031506849	0.138983051	0.592111522	4
0.666666667	0.089206066	0.769230769	0.312	0.032827832	0.126153846	0.470981678	11
0.826446281	0.079051383	0.8	0.38677686	0.029090909	0.1312	0.547067769	8
0.462962963	0.090009001	0.970873786	0.216666667	0.033123312	0.159223301	0.40901328	16
0.480769231	0.082508251	1.219512195	0.225	0.030363036	0.2	0.455363036	13
0.4784689	0.072516316	0.99009901	0.223923445	0.026686004	0.162376238	0.412985687	15
0.29154519	0.057537399	0.78125	0.136443149	0.021173763	0.128125	0.285741912	22
0.27027027	0.052246604	0.763358779	0.126486486	0.01922675	0.12519084	0.270904076	23
0.338983051	0.055187638	0.78125	0.158644068	0.020309051	0.128125	0.307078119	20
1.086956522	0.127713921	0.735294118	0.508695652	0.046998723	0.120588235	0.67628261	2
0.840336134	0.098619329	0.769230769	0.393277311	0.036291913	0.126153846	0.55572307	6
0.847457627	0.121065375	0.666666667	0.396610169	0.044552058	0.109333333	0.550495561	7
0.471698113	0.05800464	0.555555556	0.220754717	0.021345708	0.091111111	0.333211536	18
0.401606426	0.053619303	0.507614213	0.187951807	0.019731903	0.083248731	0.290932442	21
0.418410042	0.054436581	0.564971751	0.1958159	0.020032662	0.092655367	0.308503929	19
0.248756219	0.054525627	0.578034682	0.11641791	0.020065431	0.094797688	0.231281029	27
0.265957447	0.060459492	0.571428571	0.124468085	0.022249093	0.093714286	0.240431464	25
0.273224044	0.053619303	0.649350649	0.127868852	0.019731903	0.106493506	0.254094262	24

Table 5
ANOVA for Yi.

Source	DF	Seq SS	Adj SS	Adj MS	F	P	% of Contribution
A:Cutting speed	2	0.084233	0.084233	0.042116	18.26	0	16.25755622
B:Feed	2	0.368172	0.368172	0.184086	79.82	0	71.05976268
C:Cutting depth	2	0.019587	0.019587	0.009793	4.25	0.029	3.780427549
Error	20	0.046125	0.046125	0.002306			8.902446556
Total	26	0.518116					

$$Ra = 2.07667 + 0.183333 * A + 1.06278 * B + 0.0333333 * C + 0.247778 * AB - 0.123333 * AC + 0.00555556 * BC + -0.0166667 * A^2 + 0.259444 * B^2 \quad (5a)$$

$$Vibration = 13.3033 + 1.16889 * A + 1.48611 * B - 0.963333 * C + 2.26667 * AB - 3.06222 * AC - 2.43111 * BC - 0.411111 * A^2 + 0.0294444 * B^2 \quad (6)$$

$$Acoustic\ Emission = 1.05111 + 0.353889 * A - 0.08 * B - 0.0977778 * C + 0.116667 * AB - 0.224444 * AC - 0.108889 * BC + 0.119444 * A^2 + 0.112222 * B^2 \quad (7)$$

A-Cutting Speed' m/min', B- Feed Rate 'mm/min', C- Depth of cut 'mm'

3.3. MOORA analysis results

The signal-to-noise (S-N) ratio graph illustrated in Fig. 9 serves to determine the most advantageous amalgamation of input parameters. Table 3 and 4 shows the results of normalised and weighted normalisation with Yi results. The optimum combination obtained by using MOORA analysis is 80 mm/min of cutting speed 0.20 mm/min of feed rate and 0.75 mm of depth of cut. These are the overall response parameters that achieve minimum surface roughness, minimum vibration, and minimum acoustic emission.

3.4. ANOVA analysis

ANOVA revealed how process parameters affect quality attributes through an objective decision-making method based on statistical analysis. The mean square evaluation against experimental error estimates at different confidence levels identifies the significance of all process parameters. The assessment of S/N ratio variability makes it possible to identify error contributions and process parameter effects using the method of computing the standard deviation from the mean S/N ratio [38]. Table 5 shows the ANOVA table for Yi, the feed rate stands as the key factor that determines the results obtained through MOORA Yi methodology. Feed rate accounts for the highest influencing parameter with a 71.05 % contribution rate, followed by cutting speed at 16.25 %, while depth of cut holds only a 3.78 % influence rate.

Following the optimization using the MOORA method, a regression equation was produced, as shown in Eq. (8). This regression equation will be employed as a fitness function in the subsequent stages of the Whale Optimization Algorithm approaches. Using the MOORA technique, the regression equation is created as follows:

$$Yi = 1.27896 - 0.00164875 A - 2.8116 B + 0.119152 C \quad (8)$$

A-Cutting Speed' m/min', B- Feed Rate 'mm/min', C- Depth of cut 'mm'

4. Conclusion

- The present study successfully identified the optimal machining parameters, i.e., cutting speed, feed rate, and depth of cut for minimizing surface roughness, vibration, and acoustic emission during the turning of Duralumin reinforced with 5 % nano Cr_2C_3 and 2 % MoS_2.
- Using the Taguchi L27 orthogonal array design, experimental results showed that feed rate had the most significant impact on all output parameters, contributing 71.05 % to process variation, followed by cutting speed (16.25 %) and depth of cut (3.78 %) as per ANOVA analysis.
- The Artificial Neural Network (ANN) model demonstrated high prediction accuracy, making it a reliable tool for modeling complex, nonlinear machining relationships. Regression plots showed correlation coefficients above 0.94 in all stages, confirming strong alignment between experimental and predicted values.
- Multi-objective optimization using the MOORA method identified the optimal parameter combination: 80 mm/min cutting speed, 0.20 mm/rev feed rate, and 0.75 mm depth of cut, which yielded minimum surface roughness, vibration, and acoustic emission.
- The integration of ANN for prediction and MOORA for optimization offers a robust hybrid approach for enhancing the machining performance of hybrid metal matrix composites, with practical implications for improving tool life, surface integrity, and operational efficiency.

These empirical findings provide critical insights and fundamental understanding for the precision manufacturing and advanced machining of next-generation nano-reinforced aluminum matrix composite materials with enhanced surface integrity and dimensional accuracy.

CRediT authorship contribution statement

Ramesh Vellaichamy: Conceptualization. **Pugazhenthi Rajagopal:** Investigation. **Ajith Arul Daniel Selsam Chandradoss:** Methodology. **A. Geetha Selvarani:** Validation.

Declaration of competing interest

The authors declare that they have no known competing financial interests or personal relationships that could have appeared to influence the work reported in this paper.

Data availability

The data that has been used is confidential.

References

[1] W. Zhang, J. Xu, Advanced lightweight materials for automobiles: a review, Mater. Des. 221 (2022) 110994.
[2] M.Y. Khalid, R. Umer, K.A. Khan, Review of recent trends and developments in aluminium 7075 alloys and metal matrix composites (MMCs) for aircraft applications, Results Eng. 20 (2023) 101372.
[3] D.K. Sharma, D. Mahant, G. Upadhyay, Manufacturing of metal matrix composites: a state of review, Mater. Today: Proc. 26 (2020) 506–519.
[4] F. Czerwinski, Current trends in automotive light weighting strategies and materials, Materials 14 (21) (2021) 6631.
[5] C. Bell, J. Corney, N. Zuelli, D. Savings, A state of the art review of hydroforming technology: its applications, research areas, history, and future in manufacturing, Int. J. Mater. Form. 13 (2020) 789–828.
[6] P.K. Sonker, T.J. Singh, Y.K. Verma, Effect of reinforced diverse synthetic and agricultural-industrial waste materials on the microstructural and mechanical performance of hybrid metal matrix composite, Mater. Today: Proc. (2023).
[7] B.C. Kandpal, J. Kumar, H. Singh, Manufacturing and technological challenges in Stir casting of metal matrix composites–a review, Mater. Today: Proc. 5 (1) (2018) 5–10.

[8] C.H. Lauro, L. Cardoso Brandao, D. Baldo, R.A. Reis, J.P. Davim, Monitoring and processing signal applied in machining processes–a review, Measurement 58 (2014) 73–86.
[9] M. Günay, E. Yücel, Application of Taguchi method for determining optimum surface roughness in turning of high-alloy white cast iron, Measurement 46 (2) (2013) 913–919.
[10] P.G. Benardos, G.-C. Vosniakos, Predicting surface roughness in machining: a review, Int. J. Mach. Tools Manuf. 43 (8) (2003) 833–844.
[11] C. Liang, S. Yu, Y. Ma, C. Li, J. Wei, Theoretical and experimental studies of chatter in turning and machining stainless steel workpiece, Int. J. Adv. Manuf. Technol. 117 (2021) 3755–3776.
[12] R.K. Uyyuru, M.K. Surappa, S. Brusethaug, Tribological behavior of Al–Si–SiCp composites/automobile brake pad system under dry sliding conditions, Tribol. Int. 40 (2) (2007) 365–373.
[13] K.C Maddaiah, G.B. Veeresh Kumar, R. Pramod, Studies on the mechanical, strengthening mechanisms and tribological characteristics of AA7150-Al2O3 nano-metal matrix composites, J. Compos. Sci. 8 (3) (2024) 97.
[14] A.H. Karabacak, C. Aykut, Ö. Serdar, A.T. Sedat, A.Ç. Zihni, D.Y. Emre, The effects of different types and ratios of reinforcement, and machining processes on the machinability of Al2024 alloy nanocomposites, J. Compos. Mater. 57 (18) (2023) 2811–2827.
[15] M. Kok, Production and mechanical properties of Al2O3 particle-reinforced 2024 aluminium alloy composites, J. Mater. Process. Technol. 161 (3) (2005) 381–387.
[16] Y. Sahin, Optimization of testing parameters on the wear behaviour of metal matrix composites based on the Taguchi method, Mater. Sci. Eng.: A 408 (1–2) (2005) 1–8.
[17] F. Nadeem, Y. Li, B. Vucetic, M. Shirvanimoghaddam, Analysis and optimization of HARQ for URLLC. 2021 IEEE Globecom Workshops (GC Workshops), IEEE, 2021, pp. 1–6.
[18] S.V. Alagarsamy, R. Balasundaram, M. Ravichandran, V. Mohanavel, A. Karthick, S.S. Devi, Taguchi approach and decision tree algorithm for prediction of wear rate in zinc oxide-filled AA7075 matrix composites, Surf. Topogr.: Metrol. Prop. 9 (3) (2021) 035005.
[19] L. Li, S. Rong, R. Wang, S. Yu, Recent advances in artificial intelligence and machine learning for nonlinear relationship analysis and process control in drinking water treatment: a review, Chem. Eng. J. 405 (2021) 126673.
[20] A.M. Zain, H. Haron, S. Sharif, Prediction of surface roughness in the end milling machining using artificial neural network, Expert Syst. Appl. 37 (2) (2010) 1755–1768.
[21] N. Muthukrishnan, J.P. Davim, Optimization of machining parameters of Al/SiC-MMC with ANOVA and ANN analysis, J. Mater. Process. Technol. 209 (1) (2009) 225–232.
[22] A. Sahoo, A. Rout, D. Das, Response surface and artificial neural network prediction model and optimization for surface roughness in machining, Int. J. Ind. Eng. Comput. 6 (2) (2015) 229–240.
[23] G.P. Bhole, T. Deshmukh, Multi-criteria decision making (MCDM) methods and its applications, Int. J. Res. Appl. Sci. Eng. Technol. (IJRASET) 6 (5) (2018) 899–915.
[24] P. Senthil, S. Vinodh, A.K. Singh, Parametric optimisation of EDM on AlCu/TiB2 in-situ metal matrix composites using TOPSIS method, Int. J. Mach. Mach. Mater. 16 (1) (2014) 80–94.
[25] F. Khelfaoui, M.A. Yallese, S. Boucherit, N. Ouelaa, S. Belhadi, S. Ben Salem, Assessment of performance parameters in intermittent turning and multi-response optimization of machining conditions using DF, MOORA, VIKOR, and coupled NSGAII-VIKOR methods, Int. J. Adv. Manuf. Technol. 130 (11) (2024) 5665–5691.
[26] A. Kumari, B. Acherjee, Strategic selection of metal-cutting processes for thick steel plates using a hybrid decision methodology, Eng. Res. Express 6 (3) (2024) 035431.
[27] O.P. Stru, H. Enja, O.A. MatricoNa, Optimization of machining parameters in turning of hybrid aluminium-matrix (LM24–SiCp–coconut shell ash) composite, Optimization 263 (2019) 268.
[28] F. Ceritbinmez, E. Kanca, The effects of cutting parameters used in milling X153CrMoV12 cold work tool steel by end mills on surface roughness and hardness of The workpiece, Gazi Univ. J. Sci. C: Des. Technol. 10 (1) (2022) 27–38.
[29] X. Zhou, D. Qin, J. Hu, Multi-objective optimization design and performance evaluation for plug-in hybrid electric vehicle powertrains, Appl. Energy 208 (2017) 1608–1625.
[30] Q. Zhang, V. Sivalingam, M. Prasanth Balasubramanian, M. Liu, M. Sun, S. Qin, Experimental studies and multi-response optimization of cutting forces, vibrations and groove width accuracy in milling of cortical bone, Exp. Tech. (2025) 1–16.
[31] S. Agatonovic-Kustrin, R. Beresford, Basic concepts of artificial neural network (ANN) modeling and its application in pharmaceutical research, J. Pharm. Biomed. Anal. 22 (5) (2000) 717–727.
[32] S. Sun, M. Brandt, M.S. Dargusch, Characteristics of cutting forces and chip formation in machining of titanium alloys, Int. J. Mach. Tools Manuf. 49 (7–8) (2009) 561–568.
[33] M. Mia, P.R. Dey, MS. Hossain, Md.T. Arafat, Md. Asaduzzaman, Md.S. Ullah, S. M. Tareq Zobaer, Taguchi S/N based optimization of machining parameters for surface roughness, tool wear and material removal rate in hard turning under MQL cutting condition, Measurement 122 (2018) 380–391.
[34] M. Kiyak, B. Kaner, I. Sahin, B. Aldemir, O. Cakir, The dependence of tool overhang on surface quality and tool wear in the turning process, Int. J. Adv. Manuf. Technol. 51 (2010) 431–438.
[35] J.I. Hughes, A.R.C. Sharman, K. Ridgway, The effect of tool edge preparation on tool life and workpiece surface integrity, Proc. Inst. Mech. Eng., Part B: J. Eng. Manuf. 218 (9) (2004) 1113–1123.
[36] A.A. Pollock, Material brittleness and the energetics of acoustic emission, in: Experimental Mechanics on Emerging Energy Systems and Materials, Volume 5: Proceedings of the 2010 Annual Conference on Experimental and Applied Mechanics, Springer New York, New York, NY, 2011, pp. 73–79.
[37] J. Airao, G. Abhishek, C.K. Nirala, W.-J.H. Albert, Bayesian neural networks modeling for tool wear prediction in milling Al 6061 T6 under MQL conditions, Int. J. Adv. Manuf. Technol. 135 (5) (2024) 2777–2788.
[38] A.N. Haq, P. Marimuthu, R. Jeyapaul, Multi response optimization of machining parameters of drilling Al/SiC metal matrix composite using grey relational analysis in the Taguchi method, Int. J. Adv. Manuf. Technol. 37 (2008) 250–255.
[39] R. Gupta, A. Kumar Yadav, S.K. Jha, P.K. Pathak, Predicting global horizontal irradiance of north central region of India via machine learning regressor algorithms, Eng. Appl. Artif. Intell. 133 (2024) 108426.